

MIT Open Access Articles

*Degradation of Regenerated Silk
Fibroin in Soil and Marine Environments*

The MIT Faculty has made this article openly available. **Please share** how this access benefits you. Your story matters.

Citation: Zvinavashe, Augustine T, Barghouti, Zeina, Cao, Yunteng, Sun, Hui, Kim, Doyoon et al. 2022. "Degradation of Regenerated Silk Fibroin in Soil and Marine Environments." ACS Sustainable Chemistry & Engineering, 10 (34).

As Published: 10.1021/acssuschemeng.2c00949

Publisher: American Chemical Society (ACS)

Persistent URL: <https://hdl.handle.net/1721.1/150422>

Version: Author's final manuscript: final author's manuscript post peer review, without publisher's formatting or copy editing

Terms of use: Creative Commons Attribution-Noncommercial-Share Alike



1 Degradation of Regenerated Silk Fibroin in Soil and 2 Marine Environments

3 Augustine T. Zvinavashe[†], Zeina Barghouti[†], Yunteng Cao[†], Hui Sun[†], Doyoon Kim[†], Muchun
4 Liu[†], Eugene J. Lim[†] and Benedetto Marelli^{†*}

5 [†]Department of Civil and Environmental Engineering, Massachusetts Institute of Technology,
6 Cambridge, MA, 02139, United States

7 Corresponding author: Benedetto Marelli – bmarelli@mit.edu

8 KEYWORDS – silk, degradation, sea, water, soil, bacteria, environment

9 ABSTRACT

10 There is a compelling need to find new materials that meet stringent performance requirements
11 for application in food, water and agriculture industries while addressing biodegradability,
12 circular life cycle, and sustainable sourcing at scale. Regenerated silk fibroin (SF) is a structural
13 biopolymer with applications in biomedicine, optoelectronics, food, water, and agriculture.
14 Extracted from largely available *Bombyx mori* cocoons through a water-based process, SF is
15 fabricated into advanced materials that have competitive performance and merits of natural
16 origin and non-toxicity. As a protein, SF is considered slowly degradable in the human body but
17 as a material it is known to be environmentally stable, and its biodegradation is mostly unknown.
18 In this study, the degradation of SF in different soil and water environments is investigated. The
19 effects of SF polymorphism, ionic strength, and presence of microorganisms on the
20 proteinaceous material degradation are investigated. Modulation of beta sheet content allowed to
21 control the degradation rate of SF films in soil of increasing NaCl concentration. Microbial
22 activity was a key driver for silk degradation in different environmental conditions. Bacterial
23 colonization accelerated silk film degradation, process that was further enhanced by
24 encapsulation of bacteria in SF materials at the point of material assembly. Together, these data
25 show that SF biodegradation can be controlled by material design and by regulating the
26 interaction with microorganisms present in the environment.

27

28 INTRODUCTION

29 The development of new materials that combine performance with mitigation of
30 environmental impact is an instrumental step to address the challenges that humanity will face in
31 the next few decades.¹⁻³ Principles of sustainability, green chemistry, biodegradation and circular
32 life cycle have been defined as key elements in reducing environmental pollution and decreasing
33 greenhouse gas emissions while enhancing quality of life. Nonetheless, the ever increasing
34 human population pressures the AgroFood, water and energy infrastructures to rapidly rise their
35 outputs using already available, cost efficient, technological solutions, which are mostly based
36 on linear materials and resource models that follow make-take-discard practices.^{4,5} To challenge
37 these systems, several new policies are forcing stakeholders to transition to new technological
38 solutions that minimize environmental impact. In 2019, the European Chemicals Agency
39 (ECHA) proposed a wide-ranging restriction on intentional uses of microplastics in products
40 placed on the EU/EEA market to avoid or reduce their release to the environment, with non-
41 biodegradable intentionally added microplastics (IAMPs) foreseen to be completely banned from
42 the market in 2025.^{6,7} These laws require to include principles of pre-determined biodegradation
43 in polymer design and as a result new materials are under investigation to substitute the current
44 standard materials used in IAMPs for applications in cosmetics, household chemicals, and
45 agriculture, with the opportunity to expand the applications to other formats such as membranes,
46 films, thermoformed etc. While new monomers and polymers that may favor a circular life cycle
47 are investigated, an attractive option is to provide new scopes for structural biopolymers
48 extracted from natural fibers or from the waste of the food and agriculture industry.

49 Natural polymers are generally abundant, non-toxic, and biodegradable and possess chemical
50 and physical properties that allow for nano- and micro-fabrication.⁷ Of particular interest is silk,

51 a 5000-year-old textile fiber that is increasingly studied as biomaterials for biomedicine, optics,
52 photonics, water filtration, food and agriculture.⁸⁻¹¹ Silk fibroin (SF) is the structural protein
53 present in silk fibers. SF is available from sericulture through the transformation of mulberry tree
54 leaves in cocoons by the 5th instar larva of the *Bombyx mori*. In 2020, 1.1·10⁵ tons of silk cocoons
55 have been produced globally (0.1% of the whole fiber production market), with a percentage of
56 15-35% considered unreelable or pierced. SF fibers are renowned for their low diameter (brin
57 size of circa 10 μm), high flexibility, non-toxicity, and mechanical strength, with applications
58 from high-quality gowns to parachutes and suture threads. For applications beyond textile, silk
59 cocoons (both textile grade and unreelable) can be regenerated in a water suspension similar to
60 the dope present in the gland of the *Bombyx mori* larvae.¹²⁻¹⁵ In this state, SF can be considered
61 as a water-soluble polymer that can be nano- and micro-fabricated into several materials such as
62 coatings, microparticles, nanofibers, prints, hydrogels, foams, films, membranes, photonic
63 crystals, and hierarchical materials. The assembly process of SF molecules generally occurs in
64 water at mild temperature and pH conditions, allowing for the encapsulation of dopants, e.g.
65 enzymes, cells and microorganisms, nanoparticles, bioinorganics, and biomolecules that add
66 orthogonal functionalities to the final material format.¹⁶ Additionally, SF polymorphism, i.e.
67 folding of the protein in different molecular structures that range from random coils to beta-
68 sheets, regulates material solubility in water: disordered SF is readily water soluble, while an
69 ordered folding of the protein makes it water insoluble and more stable in the environment.¹⁷

70 Due to the economic importance as textile, many previous studies evaluated the degradation
71 of silk fibers under different environmental conditions.¹⁸ UV irradiation leads to the cleavage of
72 chemical bonds in the protein chains, which creates free radicals that further degrade the
73 proteinaceous material, ultimately decomposing the protein into short peptides.^{18,19} High

74 humidity and high temperature conditions are also known to accelerate silk fibers loss in
75 molecular weight and tensile strength through oxidation and hydrolysis.¹⁸ Mazibuko et al. have
76 also reported silk fiber degradation in soil and suggested that the textile degradation was mostly
77 the result of microbial activity.²⁰ Another interesting case is the maritime environment; in 1840
78 Major-General Charles Pasley, a Colonel of the Royal Engineers, recovered silk garments of
79 satin weave from the HMS Royal George, which sunk in 1782.²¹ The silk was “intact and
80 perfect”, while leather was found only in pieces and no woolen clothing was recovered in the
81 wreckage.²¹

82 Despite the extensive body of knowledge on degradation of silk textile in the environment,
83 little is known on biodegradation of regenerated SF (SF), except for the *in vivo* studies.^{22–24} This
84 is surprising as applications of SF are rapidly expanding towards nanofibrillar matrices for water
85 filtration, coatings to extend food shelf life, films for transient electronics, and microneedles for
86 foodborne pathogen sensing and for delivery of bioactive payloads in plants.^{25–33} As SF is poised
87 to become a technical material, understanding its biodegradation in different environmental
88 conditions becomes paramount to embed the material life cycle as a design parameter and to
89 comply with emerging policies that require polymers to be biodegradable with pre-determined
90 rates of mass loss. In this study, we provided a first general attempt to understand mechanisms of
91 SF degradation in the environment. Using the film format as a model, we investigated SF
92 degradation in soil, freshwater, and sea water, as a function of salt (NaCl) concentration,
93 microbial activity, and silk polymorphism. The findings provide critical knowledge to design silk
94 materials with pre-defined performance (e.g., mechanics, degradation rates) in relationship to the
95 environment in which they are deployed and to meet new environmental guidelines for
96 polymeric materials.

97 **EXPERIMENTAL SECTION**

98 An overview of the silk film degradation studies conducted in several environmental conditions
99 is depicted in **Figure 1**.

100 **Preparation of silk solutions.** *Bombyx mori* silk fibroin solutions were prepared according to
101 previously published procedures by Rockwood et al.¹⁶ Cocoons were boiled for 45 min in an
102 aqueous solution of 0.02 M Na₂CO₃, and then rinsed thoroughly with water to remove sericin
103 proteins. The extracted silk fibers were dissolved in a 9.3M LiBr solution at 60°C for 4 hours.
104 This solution was then dialyzed against Milli-Q water using Slide-a-Lyzer dialysis cassettes (3.5
105 kDa MWCO) for 72 h. The resulting SF suspension was then purified by centrifugation at 9000
106 rpm (~12,700g) over two 25-minute-long periods at 4°C.¹⁶

107 **Preparation of silk and CIAT 899 solution.** Suspensions were prepared by mixing gram
108 negative plant growth promoting rhizobacteria's (*Rhizobium tropici* CIAT 899 Martinez-Romero
109 et al. - ATCC 49672) with silk fibroin. 50% tryptic Soy Broth (Becton Dickinson, Franklin
110 Lakes, NJ, USA) was prepared by adding 500 ml of H₂O to 2.5 g Bacto-peptone (Soybean-
111 Casein Digest Medium) (Becton Dickinson, Franklin Lakes, NJ, USA), 1.5 g Yeast extract and
112 0.7 M CaCl₂ (autoclaved, working concentration dilute 100X) . The media was autoclaved for 60
113 min at 121°C. CIAT 899 was sourced and cultured in a shaker incubator at 200 rpm and 30°C up
114 to an OD600 measure of 1. Once bacteria reached an OD600 of 1, 10 ml of bacteria broth
115 solution was centrifuged at 4300 rpm for 20 min. The bacteria formed a pellet, and the
116 supernatant was discarded. Lastly, 10 ml of 6 wt% silk fibroin was pipetted into the pelleted
117 bacteria strain and uniformly mixed by thoroughly pipetting up and down.

118 **Silk fibroin film fabrication by drop casting.** 1 ml of ~7 wt% silk solution was cast on
119 polydimethylsiloxane (PDMS) sheet to obtain regular silk fibroin films. The film physico-

120 chemical and mechanical properties have been extensively studied previously.³⁴⁻³⁶ For silk
121 fibroin films embedded with *rhizobium tropici* CIAT 899, CIAT 899 was grown and centrifuged
122 as reported above. The CIAT 899 pellet was mixed with silk fibroin solution and was cast on
123 PDMS. The films were air-dried in a biological hood to control the drying rate. Once dried,
124 water insoluble silk fibroin films with a thickness of $80 \pm 10 \mu\text{m}$ and diameter of $31 \pm 2.9 \text{ mm}$.
125 were also prepared by the water annealing treatment. Water annealing (enhancement of beta-
126 sheet content) was achieved through exposure of silk fibroin films to water vapors under vacuum
127 at 22°C for 3 hours, 6 hours and 9 hours as required to obtain an average beta sheet of content of
128 44%, 50% and 54%, respectively. Water vapor drives the crystallization (beta sheet formation) of
129 silk fibroin.³⁷ .

130 **Degradation in soils.** Dulytek premium nylon 100-micron mesh bags were loaded with 6 hour
131 annealed silk fibroin films, unless stated, and sealed. The bags were then placed in soil with 25%
132 water content at standard room conditions. Soil moisture was maintained by watering the soil
133 every third day. The sealed bags were carefully taken out with tweezers at relevant time points.
134 The samples were rinsed with distilled water and air dried for 48 hours. During the drying
135 process, samples were repeatedly weighed and no further water loss was consistently measured
136 after 48 hours of drying. The degree of degradation was determined gravimetrically at $t=1, 2$
137 and 4 weeks. Initial sample mass was determined before degradation and final sample mass was
138 determined after degradation. $n=5$ samples were used for soil degradation studies and for each
139 time point different samples were used. Two factors were tested in the soil degradation studies.
140 1. Effect of silk film beta sheets content; 2. effect of varying soil salinity by varying NaCl
141 concentration in soil (0 mM, 50 mM, 100 mM and 200 mM).

142 Degradation in bacteriostasis was also investigated, by mixing 2.5% sodium azide solution into
143 the test soil (ml per g of soil) to inhibit microbial activity

144 **Degradation in water environments.** The mass of silk fibroin specimen was noted and samples
145 were added to constant volumes of NaCl solution. The silk specimen mass to NaCl solution
146 volume were kept constant for all experiments and repeats. Measurements of dissolved silk
147 fibroin (protein) in NaCl solution was used as a proxy for silk fibroin film degradation. The total
148 loss of mass from silk fibroin specimens would give a total protein content (100%) in NaCl
149 solution. Using a BCA Protein Assay kit (Sigma Aldrich), the protein content was measured for
150 each sample considered. For every experiment, n=3 was used. Seawater was purchased from
151 Worldwide Imports AWW84130 Live Nutri Seawater. The following NaCl solution
152 concentrations were used: 0 mM, 50 mM, 100 mM and 200 mM as proxy for fresh and salty
153 water.

154 **Polysaccharide detection test.** The anthrone test was performed to detect carbohydrates in
155 degraded SF film samples.³⁸ SF films and SF films with encapsulated *R. tropici* were compared
156 before and after 30 days of degradation in soil (n=5). . The films were tested before and after 30
157 days of degradation in soil (n=5). After 30 days of silk film degradation in soil, the films were
158 carefully removed from the filter bags and cleaned with a blotting paper to get rid of any
159 remaining soil residue. Each sample was weighed and added to a vial with 1 ml of distilled
160 water. 5 ml of anthrone reagent (2 mg/ml) dissolved in conc. sulfuric acid was added to each vial
161 and heated at 90°C while stirring with magnetic stir bars at 400 RPM for 17 minutes. The optical
162 density of each sample was measured using a spectrophotometer at a wavelength of 620 nm
163 (OD620) and compared to a standard curve prepared by testing standard samples with known
164 glucose concentrations.

165 **Protease activity.** *R. tropici* was grown in a broth solution as previously described. Once the
166 bacteria reached an OD600 of 1, 1 ml of the broth solution was centrifuged at 4300 rpm for 20
167 minutes and the pellet was resuspended in 30 ml of PBS solution in a 50 ml centrifuge tube and
168 incubated at room temperature. In 3-day intervals, 500 μ l samples were removed from the tube,
169 centrifuged at 4300 rpm for 10 minutes, and the supernatant was used to measure protease
170 activity using the EnzChek Protease Assay Kit (E6639 ThermoFisher Scientific). The
171 fluorescence-based assay contains casein derivatives that release red fluorescent dye-labeled
172 peptides through a protease-catalyzed hydrolysis, where the increase in fluorescence is
173 proportional to protease activity. Protease activity in units/ml can be quantified by comparing
174 against a standard curve of a protease with known activity. Fluorescence was measured on a
175 plate reader with excitation and emission wavelengths of 590 nm and 645 nm, respectively.

176 **pH changes.** A drop of universal pH indicator (1.09175 Sigma Aldrich) was added to the silk
177 solution before the drop casting step when preparing SF films and SF films loaded with *R.*
178 *tropici*, as described earlier. The films were loaded in mesh bags and placed in soil as described
179 earlier for degradation in soil. The films were taken out at relative time points for up to 14 days (t
180 = 0,2, 4, 8 and 14 days) and the color changes due to the pH indicator were observed.

181 **Fourier Transform Infrared Spectroscopy (FTIR).** Drop cast films (thin films formed by
182 dropping silk onto a flat surface followed by evaporation of the solution) were analyzed using
183 Thermo Fisher FTIR6700 Fourier Transform Infrared Spectrometer through attenuated total
184 reflection (ATR) with a germanium crystal. For each sample, 64 scans were coadded with a
185 resolution of 4 cm^{-1} , at wave numbers between 4000 and 650 cm^{-1} . The background spectra were
186 collected under the same conditions and subtracted from the scan for each sample.

187 **Scanning Electron Microscopy (SEM).** Drop cast films were freeze cracked after being dipped
188 in liquid nitrogen and analyzed with a Zeiss Merlin High-resolution scanning electron
189 microscope. Samples prepared did not charge, therefore no gold plating or any preparation of
190 samples was required. An EHT of 1.00kv was used with a 100pA probe.

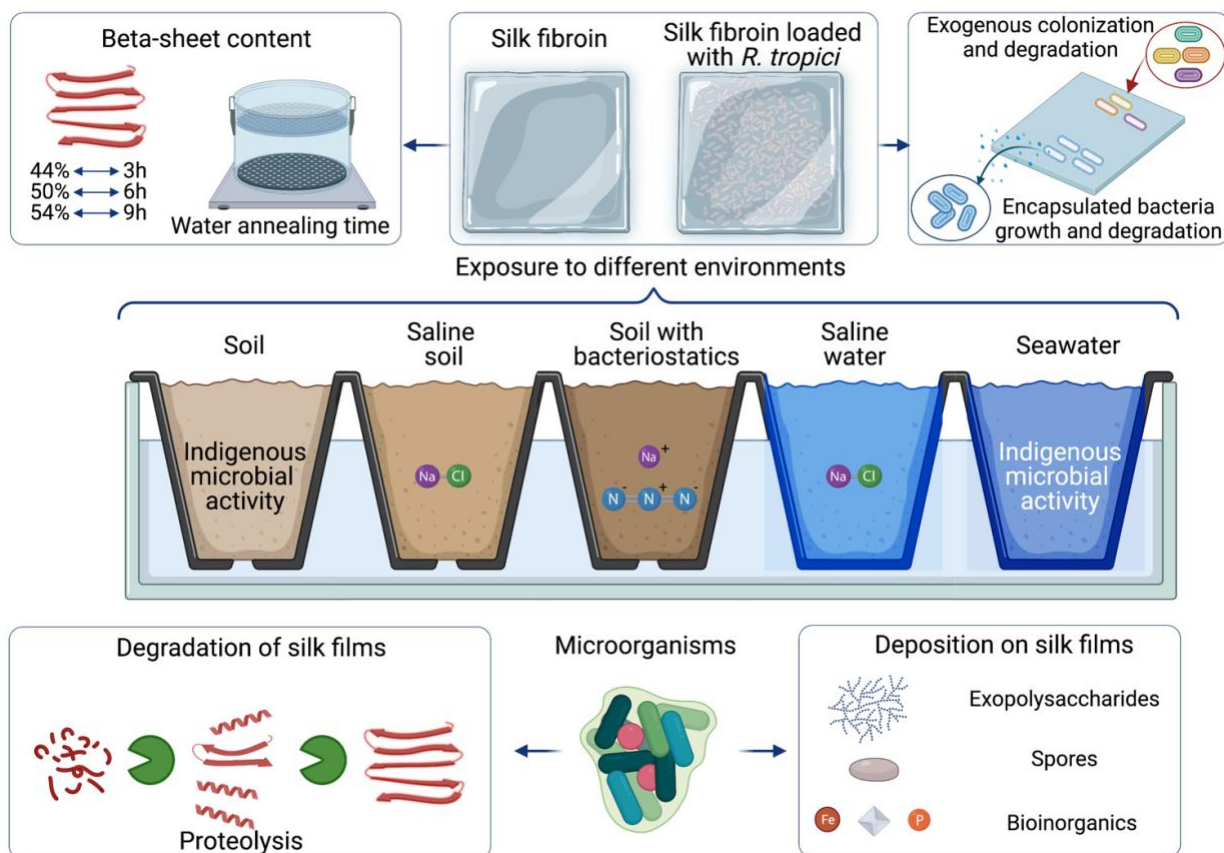
191 **Nanoindentation.** Nanoindentation measurements were performed on a Hysitron TriboIndenter
192 with a nanoDMA transducer (Bruker). Samples were indented in load control mode with a peak
193 force of 500 μN and a standard load-peak hold-unload function. Reduced modulus was
194 calculated by fitting the unloading data (with upper and lower limits being 95% and 20%,
195 respectively) using the Oliver-Pharr method and converted to Young's modulus assuming a
196 Poisson's ratio of 0.33 for all samples. Each type of sample was prepared and indented in triplets
197 to ensure good fabrication repeatability. For each sample, indentation was performed at a total of
198 49 points (7×7 grid with an increment of 20 μm in both directions) to ensure statistical reliability
199 of the modulus measurements.

200 **Statistical Analysis.** One-way ANOVA to determine statistical significance differences in
201 groups with one independent variable. Two-way ANOVA was used to determine how two
202 factors affected the response variable. For experiments in solution, the independent variable was
203 NaCl concentration. For experiments in soil, NaCl and beta-sheets content were the independent
204 variables. Post-hoc Tukey test was used to investigate significant difference in the means
205 ($p < 0.05$) of the different groups considered.

206 207 **RESULTS AND DISCUSSION**

208 In nature, cocoonase is indispensable for Lepidoptera insects breaking the sealed cocoon and it is
209 believed to be the most effective enzyme that can digest silk materials.³⁹ As human body lacks
210 cocoonase, studies of SF biodegradation have mostly focused on in vivo resorption of the protein

211 post-implant to elucidate the host-biomaterial interactions for applications in regenerative
212 medicine and drug delivery.²²⁻²⁴ These studies were conducted also in response to the definition
213 of silk fibers as non-biodegradable material by the United States Pharmacopeia, due to the
214 negligible tensile strength loss *in vivo* of silk suture threads in the first six months post implant.
215 Despite this definition, it is nowadays accepted – and supported by an extensive body of
216 literature – that silk materials are biodegradable. Several studies have, in fact, shown that
217 hydrolysis catalyzed by enzymatic activity is the major driving force for protein resorption in the
218 body, with gelatinase, chymotrypsin, trypsin and collagenase I being the most effective proteases
219 that our body produces to digest SF materials.^{40,41} Additionally, Ghezzi et al have shown, in a
220 multipocketed stroma rabbit model, how SF films polymorphism and the protein molecular
221 weight are the main parameters that modulate degradation rate, *in vivo*.²² Nonetheless, biotic and
222 abiotic factors present in environments such as soil and water are very different from the human
223 body, with major distinctions being water content, temperature, pH, microorganisms, salt
224 concentrations and mechanical stresses. Studies that generally modeled SF materials’
225 degradation were conducted with protease XIV, proteinase K, and papain and have shown SF
226 biodegradation at different pH, temperatures and when the protein is fabricated in different
227 material formats.^{40,42}



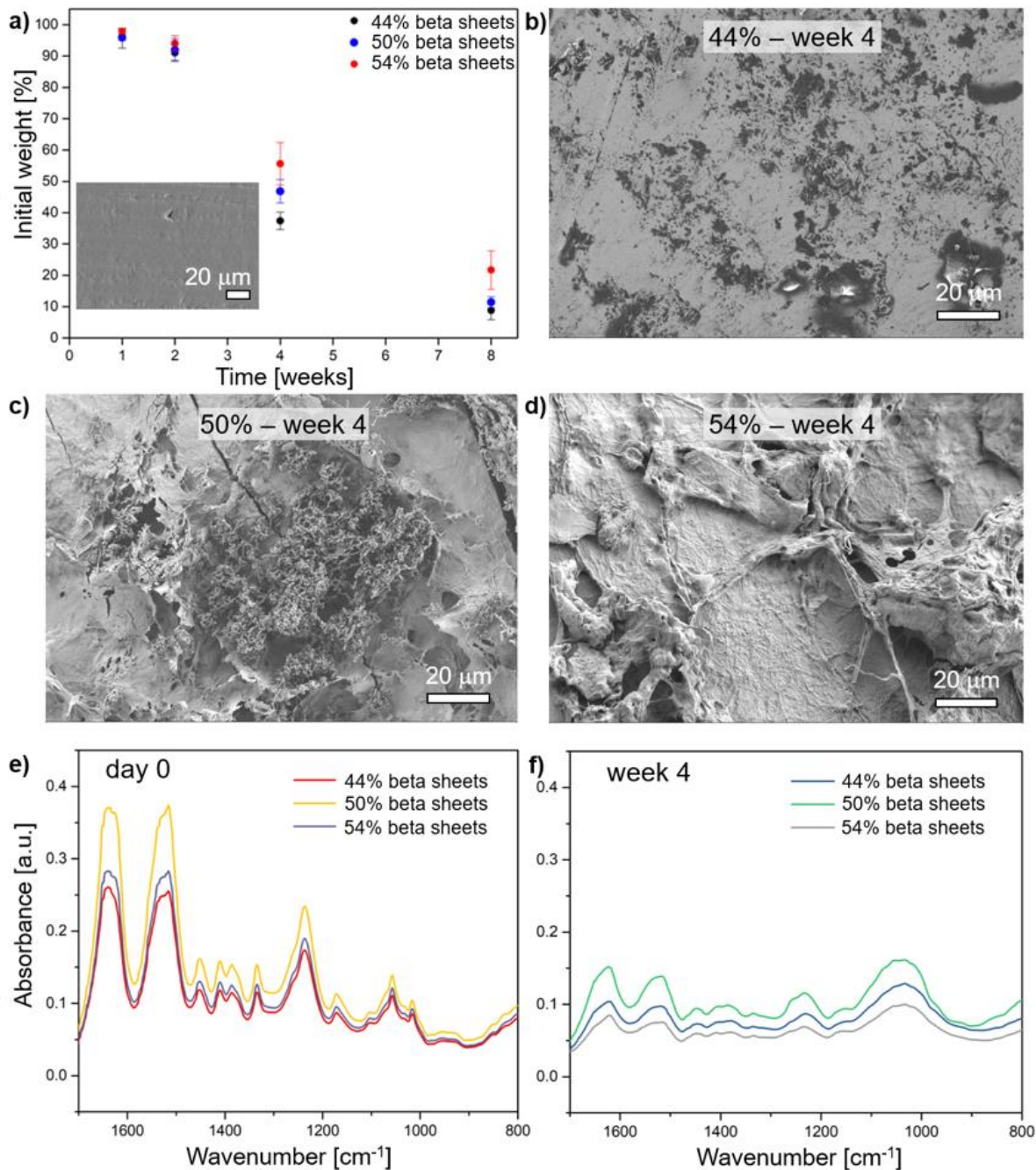
228

229 **Figure 1. Schematic of silk film degradation in several environmental conditions.** Parameters explored include
 230 protein's beta-sheet content, encapsulation of rhizobacteria, sodium chloride concentration, soil and water milieux.
 231 Resuscitation of encapsulated bacteria (i.e. indigenous) and exogenous colonization result in film degradation and
 232 deposition of exopolysaccharides, spores and bioinorganics.
 233

234 Despite this extensive body of knowledge, there is a lack of understanding of degradation
 235 phenomena of silk materials in environments such as soil and water. To address this need, we
 236 investigated silk film degradation in soil and water as a function of NaCl concentration,
 237 microbial activity, and silk polymorphism, as summarized in **Figure 1**. We used the film format
 238 due to the ease of fabrication, reproducibility of material properties and wide interest for end
 239 material applications such as coating, membrane, packaging, and substrate for transient
 240 electronics.^{28,30–32,43,44} SF polymorphism was modulated using water annealing post processing,
 241 which allows to slowly drive a disordered to ordered conformational change in silk fibroin
 242 molecules from random coils to beta-sheet structures through exposure to water vapors.⁴⁵ SF

243 films with a thickness of $80 \pm 10 \mu\text{m}$ were exposed to water vapors for 3, 6 and 9 hours to obtain
244 an average beta sheet content of 44%, 50% and 54%, respectively. To investigate the effects
245 of microbial activity on the degradation profile, *Rhizobium tropici* CIAT 899 – a strain of
246 endosymbiotic, nitrogen fixing bacteria commonly used as biofertilizer for legumes – were
247 encapsulated in SF film at the point of material assembly.³² The effects of CIAT 899
248 encapsulation on SF degradation in soil was compared to negative controls composed of neat SF
249 films and was studied as a function of soil NaCl concentration, presence of bacteriostats, and
250 protein beta sheet content. Additionally, SF films degradation was studied in water at increasing
251 sodium chloride concentration and in sea water.

252 **Figure 2** summarizes the influence of beta sheet content on SF film degradation in soil.
253 ANOVA test conducted on measurements of weight loss over time indicated that a statistically
254 significant difference of material degradation occurred across time ($p < 0.05$) and across different
255 beta sheet content ($p < 0.05$). At week 4, silk fibroin films lost between 50 and 60% of their
256 original weight. At week 8, the films were heavily degraded (between 8 and 20% of the original
257 weight remained) and lost their structural integrity (Figure 2a). SEM was used to investigate SF
258 films morphology at week 4 of exposure to soil.



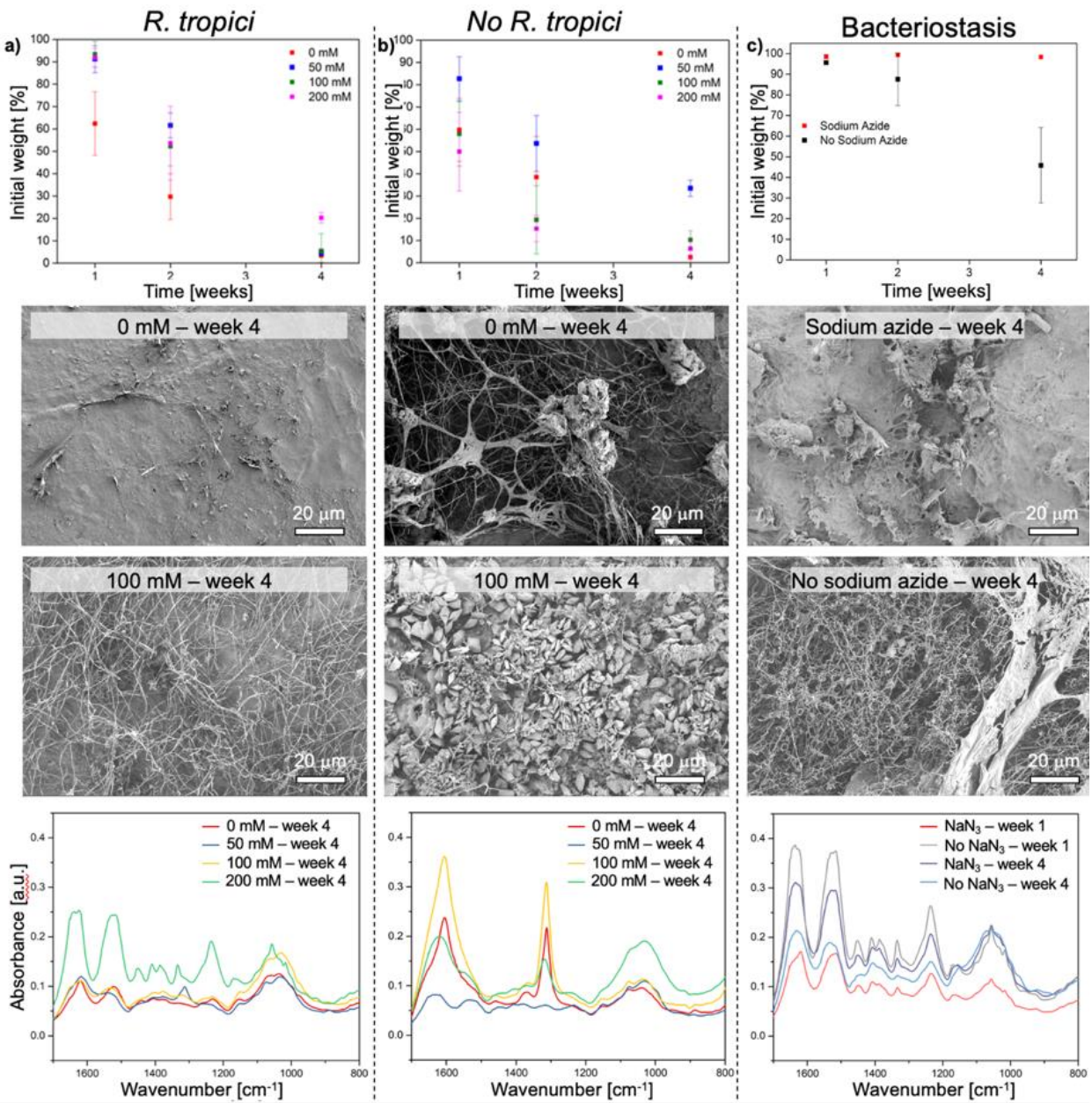
259

260 **Figure 2. Influence of beta sheet content on silk fibroin film degradation in soil.** Beta sheets content in silk
 261 fibroin films was modulated with post-processing water annealing. a) Silk fibroin film degradation profile as a
 262 function of different beta sheets content. Statistically significant difference of films degradation occurred across time
 263 ($p < 0.05$) and across different beta sheets content ($p < 0.05$). b-d) SEM images of silk fibroin film with increasing beta sheet
 264 content at week 4 in soil. When compared to a 50% beta sheet silk film at day 0, SEM image inset in panel a),
 265 silk films showed surface erosion and deposition of exogenous materials. Samples at week 8 were too degraded to
 266 be analyzed. e-f) ATR-FTIR analysis of silk fibroin films of increasing beta sheets content at (e) day 0 and (f) week
 267 4 in soil. Amide I (1700-1600 cm⁻¹) peak is dominated by random coil (1643 cm⁻¹) and beta sheet (1622 cm⁻¹)
 268 vibrations. The fingerprint region of silk is in the (1200-900 cm⁻¹) is visible at day 0 but altered at week 4. C-C and
 269 C-O stretching and CH₃ bending vibrations in the 1100-1000 cm⁻¹ region present at week 4 are typical of
 270 polysaccharides.

271
272 For all the levels of beta sheet content considered, SF films showed surface degradation and
273 deposition of exogenous material (Figure 2b-d). SF films at day 0 are in fact generally smooth
274 with no features on the surface identifiable at the micrometer scale (Figure 2a, inset). We
275 speculate that deposition of exogenous material and surface erosion can be attributed to
276 microbial activity. To further investigate chemical deterioration of the films surface post
277 treatment in soil, we conducted ATR-FTIR analysis on silk films of increasing beta sheet content
278 at day 0 (Figure 2e) and compared the spectra with the one obtained at week 4 (Figure 2f).⁴⁶
279 Amide I ($1700\text{-}1600\text{ cm}^{-1}$) analysis of samples at week 4 depicted an increase in beta sheet
280 content (1622 cm^{-1}) when compared to the day 0 controls.⁴⁶ Silk fibroin degradation occurs in
281 molecules that have a non-ordered configuration (1643 cm^{-1}), first. Hence, the contribution in the
282 Amide I of non-ordered fibroin molecules is reduced over time, leaving silk with mostly beta
283 sheet structure. The fingerprint region ($1200\text{-}900\text{ cm}^{-1}$) of silk fibroin is also altered at week 4
284 due to the deposition of exogenous biopolymers, e.g. exopolysaccharides (EPS) symmetric CH_3
285 bending in the $1100\text{-}1000\text{ cm}^{-1}$ region.⁴⁷ Surprisingly, silk films developed a slight pinkish color
286 at week 4 (Supporting Figure S1), which may be due to deposition of bioinorganics on the
287 surface of silk. ICP-MS analysis of silk samples at week 4 of soil treatment showed in fact
288 accumulation of iron in silk films (Supporting Table S1).

289 The influence of biofertilizers, sodium chloride concentration and bacteriostasis on silk
290 fibroin film degradation was also studied in soil (**Figure 3**). *Rhizobium spp.* are soil-dwelling α -
291 Proteobacteria that can fix nitrogen in a symbiotic relationship with leguminous plants and that
292 can boost seed germination and mitigate biotic and abiotic stressors.⁴⁸ As biofertilizers for
293 precision and restorative agriculture, *Rhizobium spp.* hold a high potential as their use would
294 decrease the need to deploy nitrogen fertilizers, the production of which accounts for 1-2% of the

295 world energy consumption and ~3-5% of the natural gas produced globally.^{49,50} However,
 296 preservation of *Rhizobium spp.* outside the soil is challenging.⁵¹ Building on previous studies that
 297 have reported *Rhizobium* encapsulation in silk materials as an effective strategy to preserve and
 298 deliver biofertilizers, we encapsulated *Rhizobium tropici* CIAT 899 in silk fibroin films to study
 299 the effects of indigenous bacterial activity on material degradation when compared to silk fibroin
 300 film controls (Figure 3a and b, respectively).³²



301

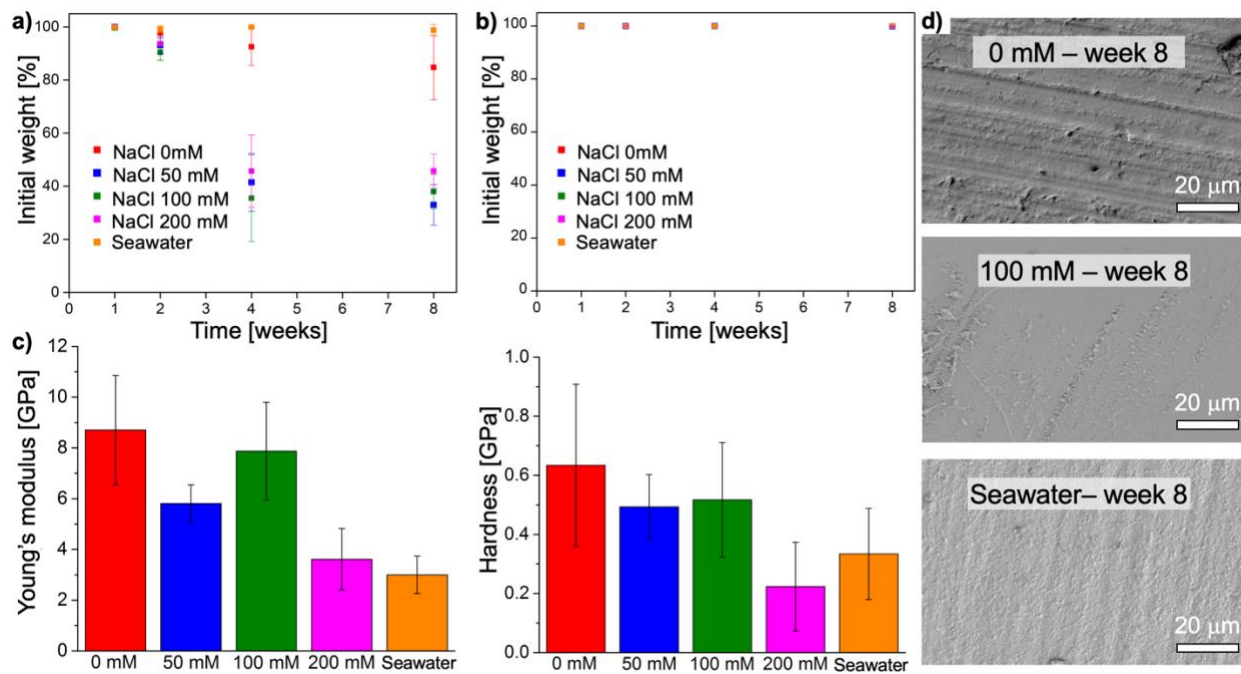
302 **Figure 3. Influence of biofertilizers, soil sodium chloride concentration and bacteriostasis on silk fibroin film**
303 **degradation in soil.** a-b) Encapsulation in silk fibroin films of (a) biofertilizers such as *Rhizobium tropici* accelerates
304 material degradation when compared to (b) silk fibroin film controls. Soil sodium chloride concentration also affects
305 silk film degradation over time ($p < 0.05$). ATR-FTIR spectra suggest the deposition of exopolysaccharides on the
306 surface on silk films. c) Effect of bacteriostasis on silk film degradation. When sodium azide (NaN_3) is added to soil,
307 silk fibroin degradation is hindered, indicating that silk degradation in soil is prevalently microbial ($p < 0.05$).

308 *R. tropici* were encapsulated in silk films at the point of material assembly and preserved in dry
309 state. As saprophytes, rhizobia survive in a complex microbial community by adopting an
310 oligotrophic lifestyle.⁵² Upon exposure to the moist soil, *R. tropici* activity increases and it can
311 be speculated that proteases released by the bacteria and local changes in pH induced by
312 bacterial activity accelerate silk fibroin degradation.^{53,54} To test this hypothesis, we monitored
313 over time the expression of proteases in *R. tropici* cultured in PBS and found a time-dependent
314 increase in proteolytic enzymes content in the bacterial culture media (Supporting Figure S2a). A
315 one-way ANOVA test was performed and showed a significant difference between the groups,
316 followed by a Tukey test which showed a significant difference ($p < 0.05$) between day 0 and day
317 9, as well as between day 3 and day 9. The linear increase in the protease activity of *R. Tropici*
318 may indicate that *R. tropici* constantly express proteases. Additionally, we studied pH changes
319 in silk films encapsulating *R. tropici* and degrading in soil by adding a universal pH indicator to
320 the silk materials at the point of film assembly. The universal pH indicator dye is incorporated in
321 the films and undergoes a color change when the pH of the environment shifts. Over time, the
322 dye indicated that the presence of *R. tropici* in silk films generated a more acidic environment,
323 when compared to the films left in soil with no bacteria encapsulated (Supporting Figure S2b).
324 Also, the encapsulation of non-motile bacteria in SF films may have induced a bulk degradation
325 when compared to surface erosion that occurs during the exogenous colonization of silk fibroin
326 films exposed to soil microorganisms. *R. tropici* encapsulated films were in fact more degraded
327 over time compared to control films, when there was no NaCl treatment. Anthrone test was used
328 to quantify the amount of carbohydrates present in silk films degraded in soil for 30 days when

329 compared to the as made ones. The carbohydrates content for silk films with and without *R.*
330 *tropici* was also measured. The amount of carbohydrates was statistically significant higher
331 ($p < 0.05$) after 30 days of exposure to soil and in silk films containing the biofertilizer ($p < 0.05$)
332 (Supporting Table S2). As the increased presence of carbohydrates in silk films degrading in soil
333 can be due to the deposition of EPS, SEM analysis was performed on the surface of silk films
334 and showed the deposition of nanofibrillar matrices on the surfaces of silk films loaded with *R.*
335 *tropici*. These matrices were identified as biopolymers rich in saccharides from FTIR analysis
336 (stretching vibration of the carboxylate group at $1700\text{-}1500\text{ cm}^{-1}$, and C–C and C–O stretching
337 and symmetric CH_3 bending in the $1100\text{-}1000\text{ cm}^{-1}$ region). Together, these analyses suggest that
338 EPS were deposited on silk films. Nanofibrils were more evident on silk films at higher soil
339 sodium chloride concentration (Figure 3a), in agreement with previous studies that showed an
340 increased EPS synthesis in response to abiotic stressors.⁴⁷ Interestingly, the samples that were
341 not loaded with *R. tropici* and exposed to soil at increasing sodium chloride concentration
342 showed a more prominent deposition of nanofibrils on the film surface at week 4, when
343 compared to the samples loaded with the biofertilizers, even though film degradation remained
344 comparable to *R. tropici* films at 100 mM NaCl concentration. This result may suggest that an
345 exogenous colonization on the surface of the silk films was more prominent when endogenous *R.*
346 *tropici* were not encapsulated in the degrading materials or that the presence of biofertilizers in
347 silk films partially inhibits nanofibrils deposition on the films' surface (Figure 3b). Nonetheless,
348 more studies are necessary to elucidate microbial communities' interactions at the silk-soil
349 interface. Sodium chloride concentration affected silk film degradation over time ($p < 0.05$) and
350 SEM and ATR-FTIR analyses indicated the deposition of nanofibrillar biopolymers on the
351 surface on silk films. Additionally, at high sodium chloride concentrations (i.e. 100mM),

352 electron microscopy revealed the presence of spores on the surface of the films. The experiment
353 of *R. tropici*-loaded SF films degradation in soil was repeated upon addition of a bacteriostatic
354 agent such as sodium azide (NaN_3) to soil (Figure 3c). Sodium azide is a very common
355 bacteriostat that inhibits most gram-negative bacteria, including *R. tropici*, but that is less
356 effective with gram-positive bacteria (streptococci, pneumococci, lactobacilli, etc.).⁵⁵ Exposure
357 of *R. tropici*-loaded SF films resulted in a decrease degradation rate and a reduced deposition of
358 nanofibrillar biopolymers on the surface of the silk materials. Together, these experiments
359 showed that SF film degradation in soil is driven by microbial activity and that the degradation
360 profile is influenced by biotic (i.e. microbial communities) and abiotic (i.e. salt concentration)
361 environmental parameters as well as silk properties (i.e. polymorphism). In particular, NaCl
362 concentration – for the ranges studied - positively affected bacterial-driven degradation, also
363 indicating an interplay between the material, biotic and abiotic parameters. A higher NaCl
364 concentration may in fact promote the biological activity by maintaining a suitable osmotic
365 pressure in the soil. However, future studies will be required to better understand the effects of
366 soil salinity on the proteolytic activity of microbial communities in soil.

367



368

369 **Figure 4 – Silk fibroin film biodegradation in water environments.** Effects of increasing sodium chloride
 370 concentration on silk fibroin film biodegradation in water for films a) loaded with *R. tropici* and b) not loaded with
 371 the biofertilizers. Seawater and deionized water are used as controls. c) Negligible weight loss was measured in
 372 seawater for the 8 weeks of the study, although a statistically significant decrease ($p < 0.05$) in the mechanical properties
 373 (i.e. Young modulus and hardness) of the films was measured through nanoindentation, when compared to films at
 374 week 8 of exposure to 0, 50 and 100 mM of NaCl solution. d) SEM microscopy of *R. tropici*-loaded silk films at week
 375 8.

376 There is an increasing interest in investigating the degradation of polymers (synthetic and
 377 natural) in water. From an environmental impact perspective, accumulation of synthetic
 378 materials in freshwater and seawater produces 4.8-12.7 million tons of plastic waste every year,
 379 with 80% of marine debris originating from land and being transported to seas via water
 380 streams.^{56,57} Additionally, biodegradation of biopolymers (typically polysaccharides such as
 381 alginate, chitin, and starch) in freshwater and marine environment by heterotrophic microbial
 382 communities has global implications on biogeochemical carbon cycles and its effects on climate
 383 change. For structural proteins, biodegradation of ubiquitous tissue components like collagen is
 384 well documented, while little is known on the hydrolysis rate of silks synthesized by arthropods
 385 to perform in freshwater and seawater (e.g. spider silk of aquatic spiders *Argyroneta aquatica*
 386 and *Desis marina*, respectively). **Figure 4** illustrates SF film biodegradation in water

387 environments. For freshwater, the effects of increasing sodium chloride concentration (0-200
388 mM) were investigated when *R. tropici* were encapsulated in the silk material at the point of
389 material assembly and using non-loaded SF films as control (Figure 4a and b, respectively).
390 Degradation of SF films loaded and non-loaded with *R. tropici* was also investigated in seawater.
391 SF mass loss measurements over time showed that *R. tropici* induced silk fibroin biodegradation
392 in water and the degradation rate was higher at sodium chloride concentrations that allow for the
393 biofertilizers survival (NaCl 50-200mM). Negligible weight loss was in fact measured in
394 deionized water (NaCl = 0 mM). For seawater, minor weight loss was also measured for the 8
395 weeks of the study; this may be caused by the limited number of microorganism present in
396 seawater when compared to soil and by the low survival of *R. tropici* in a non-natural
397 environment for the rhizobacteria. However, a statistically significant decrease ($p < 0.05$) in the
398 mechanical properties (i.e. Young's modulus and hardness) of the SF films exposed to seawater
399 was measured with nanoindentation, when compared to SF films at week 8 of exposure to 0, 50,
400 and 100 mM of NaCl solution (Figure 4c), which may suggest that hydrolysis causes a decrease
401 in the protein MW in the time frame considered. SEM microscopy of *R. tropici*-loaded silk films
402 at week 8 showed no sign of biopolymers deposition on the surface when exposed to deionized
403 water (NaCl 0 mM) and in seawater, while nanofibrous biopolymers were visible in samples
404 exposed to NaCl 100 mM solution. Together, these results suggest that degradation of SF films
405 in seawater and freshwater requires the presence of active heterotrophic bacteria that possess the
406 capability of digesting the silk material. The higher silk degradation rate in soil when compared
407 to freshwater and seawater may be due the higher density of bacteria in soil (10^8 - 10^9 bacteria / g
408 of soil) when compared to seawater (10^5 bacteria / g of surface sea water) and freshwater (10^3 -
409 10^5 bacteria / g of freshwater). Additionally, soil dwelling microorganisms may have evolved to

410 better digest structural proteins produced by terrestrial organisms when compared to water
411 counterparts; e.g. Protease XIV produced by *Streptomyces griseus*, a gram-positive species of
412 bacteria commonly found in soil, is a mixture of at least three caseinolytic activities and one
413 aminopeptidase activity and is a well-known for its efficacy in degrading silk materials.

414

415 **CONCLUSIONS**

416 In this manuscript, we report for the first time the degradation of silk fibroin films in soil and water
417 environment as a function of abiotic and biotic factors such as sodium chloride concentration,
418 presence of biofertilizers, and bacteriostasis. The effects of silk fibroin polymorphism on
419 degradation in soil was also investigated and showed that beta sheet content can be used to
420 modulate silk fibroin film biodegradation rate. Microbial activity is a main driving force for silk
421 fibroin film degradation in soil, mainly due to the production of proteases, and results in the
422 complete degradation of the silk materials considered in soil in 8 weeks. When bacteriostats were
423 added to the soil, biodegradation was hindered but not stopped. Further, incorporation of
424 biofertilizers in silk fibroin films at the point of material assembly accelerated the material
425 degradation, promoting a bulk degradation whereas biodegradation through microbial colonization
426 from soil resulted in a surface degradation. Studies of biodegradation in freshwater and seawater
427 environments indicated slower biodegradation profiles, when compared to the measurements
428 obtained in soil, even when bacteriostats were added. Particularly interesting was the case of
429 exposure to seawater, resulting in <10% of weight loss in 8 weeks. Given the rising need to predict
430 materials' biodegradation in the environment and to embed circular life principles in the design of
431 technical innovations, this study will provide the basis to engineer silk fibroin materials for
432 applications in food, energy, water, and agriculture.

433 ASSOCIATED CONTENT

434 Supporting Information is available and show: microscopic pictures of degraded silk fibroin film
435 at week 4 of treatment in soil, the result of ICP-MS analysis conducted on the same specimen,
436 the results of the Anthrone test, expression of proteases in *R. tropici* and pH changes within silk
437 films degrading in soil.

438 AUTHOR INFORMATION

439 **Corresponding Author**

440 * Benedetto Marelli – bmarelli@mit.edu

441 **Author Contributions**

442 Augustine T. Zvinavashe and Zeina Barghouti contributed equally. The manuscript was written
443 through contributions of all authors. All authors have given approval to the final version of the
444 manuscript.

445 **Funding Sources**

446 The authors acknowledge OCP S.A. and Université Mohammed VI Polytechnique-MIT Research
447 Program. This work was partially supported by the Office of Naval Research (Awards
448 N000142112402 and N000141912317) and the National Science Foundation (Award CMMI-
449 1752172)

450 ACKNOWLEDGMENT

451 We acknowledge Miguel Lara for *R. tropici* CIAT 899-GFP from Universidad Nacional
452 Autonoma de Mexico. The authors acknowledge OCP S.A. and Université Mohammed VI
453 Polytechnique-MIT Research Program. This work was partially supported by the Office of Naval
454 Research (Awards N000142112402 and N000141912317) and the National Science Foundation

455 (Award CMMI-1752172). B.M. acknowledges a Paul M. Cook Career Development
456 Professorship and a Singapore Research Professorship.

457

458

459

460 CONFLICT OF INTEREST

461 BM is co-founder of Mori, Inc, a company that develops silk-based technologies to prolong food
462 shelf life. BM and ATZ are co-inventors on IP positions that protect the use of silk-based materials
463 to deliver biofertilizers in the soil.

464

465 REFERENCES

- 466 (1) Worrell, E.; Allwood, J.; Gutowski, T. The Role of Material Efficiency in Environmental
467 Stewardship. **2016**. <https://doi.org/10.1146/annurev-environ-110615-085737>.
- 468 (2) Chung, Y. H.; Church, D.; Koellhoffer, E. C.; Osota, E.; Shukla, S.; Rybicki, E. P.;
469 Pokorski, J. K.; Steinmetz, N. F. Integrating Plant Molecular Farming and Materials
470 Research for Next-Generation Vaccines. *Nature Reviews Materials* **2021**, 1–17.
471 <https://doi.org/10.1038/s41578-021-00399-5>.
- 472 (3) Sikder, A.; Pearce, A. K.; Parkinson, S. J.; Napier, R.; O'Reilly, R. K. Recent Trends in
473 Advanced Polymer Materials in Agriculture Related Applications. *ACS Applied Polymer*
474 *Materials* **2021**, 3 (3), 1203–1217. <https://doi.org/10.1021/ACSAPM.0C00982>.
- 475 (4) Islam, S. M. F.; Karim, Z. World's Demand for Food and Water: The Consequences of
476 Climate Change. *Desalination - Challenges and Opportunities* **2019**.
477 <https://doi.org/10.5772/INTECHOPEN.85919>.
- 478 (5) *4 ways green chemistry is helping make the world a better place | World Economic*
479 *Forum*. [https://www.weforum.org/agenda/2016/10/4-ways-green-chemistry-is-helping-](https://www.weforum.org/agenda/2016/10/4-ways-green-chemistry-is-helping-make-the-world-a-better-place/)
480 [make-the-world-a-better-place/](https://www.weforum.org/agenda/2016/10/4-ways-green-chemistry-is-helping-make-the-world-a-better-place/) (accessed 2022-01-23).
- 481 (6) Benfenati, V.; Toffanin, S.; Chieco, C.; Sagnella, A.; Di Virgilio, N.; Posati, T.; Varchi,
482 G.; Natali, M.; Ruani, G.; Muccini, M.; Rossi, F.; Zamboni, R. Silk Fibroin Based
483 Technology for Industrial Biomanufacturing. In *Factories of the Future: The Italian*
484 *Flagship Initiative*; Springer International Publishing, 2019; pp 409–430.
485 https://doi.org/10.1007/978-3-319-94358-9_19.
- 486 (7) Amobonye, A.; Bhagwat, P.; Singh, S.; Pillai, S. Plastic Biodegradation: Frontline
487 Microbes and Their Enzymes. *Science of The Total Environment* **2021**, 759, 143536.
488 <https://doi.org/10.1016/J.SCITOTENV.2020.143536>.
- 489 (8) Marelli, B. Biomaterials for Boosting Food Security. *Science (1979)* **2022**, 376 (6589),
490 146–147. <https://doi.org/10.1126/science.abo4233>.

- 491 (9) Zhou, Z.; Zhang, S.; Cao, Y.; Marelli, B.; Xia, X.; Tao, T. H. Engineering the Future of
492 Silk Materials through Advanced Manufacturing. *Advanced Materials* **2018**, *30* (33),
493 1706983. <https://doi.org/10.1002/adma.201706983>.
- 494 (10) Sun, H.; Marelli, B. Growing Silk Fibroin in Advanced Materials for Food Security. *MRS*
495 *Communications* **2021**. <https://doi.org/10.1557/s43579-020-00003-x>.
- 496 (11) Sun, H.; Cao, Y.; Kim, D.; Marelli, B. Biomaterials Technology for AgroFood Resilience.
497 *Advanced Functional Materials* **2022**, *In press*.
- 498 (12) Wang, Y.; Guo, J.; Zhou, L.; Ye, C.; Omenetto, F. G.; Kaplan, D. L.; Ling, S. Design,
499 Fabrication, and Function of Silk-Based Nanomaterials. *Advanced Functional Materials*
500 **2018**, *28* (52), 1805305. <https://doi.org/10.1002/ADFM.201805305>.
- 501 (13) Plaza, G. R.; Corsini, P.; Pérez-Rigueiro, J.; Marsano, E.; Guinea, G. v.; Elices, M. Effect
502 of Water on Bombyx Mori Regenerated Silk Fibers and Its Application in Modifying
503 Their Mechanical Properties. *Journal of Applied Polymer Science* **2008**, *109* (3), 1793–
504 1801. <https://doi.org/10.1002/APP.28288>.
- 505 (14) Kim, S. H.; Nam, Y. S.; Lee, T. S.; Park, W. H. Silk Fibroin Nanofiber. Electrospinning,
506 Properties, and Structure. *Polymer Journal* *2003* **35**:2 **2003**, *35* (2), 185–190.
507 <https://doi.org/10.1295/polymj.35.185>.
- 508 (15) Vepari, C.; Kaplan, D. L. Silk as a Biomaterial. *Progress in Polymer Science* **2007**, *32* (8–
509 9), 991–1007. <https://doi.org/10.1016/J.PROGPOLYMSCI.2007.05.013>.
- 510 (16) Rockwood, D. N.; Preda, R. C.; Yücel, T.; Wang, X.; Lovett, M. L.; Kaplan, D. L.
511 Materials Fabrication from Bombyx Mori Silk Fibroin. *Nature Protocols* **2011**, *6* (10),
512 1612–1631. <https://doi.org/10.1038/nprot.2011.379>.
- 513 (17) Marelli, B.; Patel, N.; Duggan, T.; Perotto, G.; Shirman, E.; Li, C.; Kaplan, D. L.;
514 Omenetto, F. Programming Function into Mechanical Forms by Directed Assembly of
515 Silk Bulk Materials. *Proc Natl Acad Sci U S A* **2017**, *114* (3), 451–456.
516 <https://doi.org/10.1073/pnas.1612063114>.
- 517 (18) Vilaplana, F.; Nilsson, J.; Sommer, D. V. P.; Karlsson, S. Analytical Markers for Silk
518 Degradation: Comparing Historic Silk and Silk Artificially Aged in Different
519 Environments. *Analytical and Bioanalytical Chemistry* **2015**, *407* (5), 1433–1449.
520 <https://doi.org/10.1007/s00216-014-8361-z>.
- 521 (19) Matsuhira, T.; Yamamoto, K.; Osaki, S. Effects of UV Irradiation on the Molecular
522 Weight of Spider Silk. *Polymer Journal* *2013* **45**:11 **2013**, *45* (11), 1167–1169.
523 <https://doi.org/10.1038/pj.2013.41>.
- 524 (20) Mazibuko, M.; Ndumo, J.; Low, M.; Ming, D.; Harding, K. Investigating the Natural
525 Degradation of Textiles under Controllable and Uncontrollable Environmental Conditions.
526 *Procedia Manufacturing* **2019**, *35*, 719–724.
527 <https://doi.org/10.1016/J.PROMFG.2019.06.014>.
- 528 (21) Article CS117993292. *The Times*. London October 12, 1840.
- 529 (22) Lu, Q.; Zhang, B.; Li, M.; Zuo, B.; Kaplan, D. L.; Huang, Y.; Zhu, H. Degradation
530 Mechanism and Control of Silk Fibroin. *Biomacromolecules* **2011**, *12*, 1080–1086.
531 <https://doi.org/10.1021/bm101422j>.
- 532 (23) Guarino, V.; Benfenati, V.; Cruz-Maya, I.; Saracino, E.; Zamboni, R.; Ambrosio, L.
533 Instructive Proteins for Tissue Regeneration. *Functional 3D Tissue Engineering Scaffolds:*
534 *Materials, Technologies, and Applications* **2018**, 23–49. [https://doi.org/10.1016/B978-0-](https://doi.org/10.1016/B978-0-08-100979-6.00002-1)
535 [08-100979-6.00002-1](https://doi.org/10.1016/B978-0-08-100979-6.00002-1).

- 536 (24) Tao, H.; Kaplan, D. L.; Omenetto, F. G. Silk Materials - A Road to Sustainable High
537 Technology. *Advanced Materials*. John Wiley & Sons, Ltd June 5, 2012, pp 2824–2837.
538 <https://doi.org/10.1002/adma.201104477>.
- 539 (25) Li, A. B.; Kluge, J. A.; Guziewicz, N. A.; Omenetto, F. G.; Kaplan, D. L. Silk-Based
540 Stabilization of Biomacromolecules. *J Control Release* **2015**, *219*, 416–430.
541 <https://doi.org/10.1016/j.jconrel.2015.09.037>.
- 542 (26) Kluge, J. A.; Li, A. B.; Kahn, B. T.; Michaud, D. S.; Omenetto, F. G.; Kaplan, D. L. Silk-
543 Based Blood Stabilization for Diagnostics. *Proceedings of the National Academy of*
544 *Sciences* **2016**, *113* (21), 5892 LP – 5897. <https://doi.org/10.1073/pnas.1602493113>.
- 545 (27) Marelli, B.; Brenckle, M. A.; Kaplan, D. L.; Omenetto, F. G. Silk Fibroin as Edible
546 Coating for Perishable Food Preservation. *Scientific Reports* **2016**, *6* (51), 0–1.
547 <https://doi.org/10.1038/srep25263>.
- 548 (28) Sun, H.; Marelli, B. Growing Silk Fibroin in Advanced Materials for Food Security. *MRS*
549 *Communications* **2021**, 1–15. <https://doi.org/10.1557/s43579-020-00003-x>.
- 550 (29) Ruggeri, E.; Kim, D.; Cao, Y.; Farè, S.; de Nardo, L.; Marelli, B. A Multilayered Edible
551 Coating to Extend Produce Shelf Life. *ACS Sustainable Chemistry and Engineering* **2020**,
552 *8* (38), 14312–14321. <https://doi.org/10.1021/acssuschemeng.0c03365>.
- 553 (30) Kim, D.; Cao, Y.; Mariappan, D.; Bono, M. S.; Hart, A. J.; Marelli, B. A Microneedle
554 Technology for Sampling and Sensing Bacteria in the Food Supply Chain. *Advanced*
555 *Functional Materials* **2021**, *31* (1), 2005370. <https://doi.org/10.1002/adfm.202005370>.
- 556 (31) Zvinavashe, A. T.; Laurent, J.; Mhada, M.; Sun, H.; Fouda, H. M. E.; Kim, D.; Mouhib,
557 S.; Kouisni, L.; Marelli, B. Programmable Design of Seed Coating Function Induces
558 Water-Stress Tolerance in Semi-Arid Regions. *Nature Food* **2021**, *2* (7), 485–
559 493. <https://doi.org/10.1038/s43016-021-00315-8>.
- 560 (32) Zvinavashe, A. T.; Lim, E.; Sun, H.; Marelli, B. A Bioinspired Approach to Engineer
561 Seed Microenvironment to Boost Germination and Mitigate Soil Salinity. *Proc Natl Acad*
562 *Sci U S A* **2019**, *116* (51), 25555–25561. <https://doi.org/10.1073/pnas.1915902116>.
- 563 (33) Cao, Y.; Lim, E.; Xu, M.; Weng, J. K.; Marelli, B. Precision Delivery of Multiscale
564 Payloads to Tissue-Specific Targets in Plants. *Advanced Science* **2020**, *7* (13), 1903551.
565 <https://doi.org/10.1002/advs.201903551>.
- 566 (34) Lawrence, B. D.; Omenetto, F.; Chui, K.; Kaplan, D. L. Processing Methods to Control
567 Silk Fibroin Film Biomaterial Features. *Journal of Material Science* **2008**, *43*, 6967–6985.
- 568 (35) Bressner, J. E.; Marelli, B.; Qin, G.; Klinker, L. E.; Zhang, Y.; Kaplan, D. L.; Omenetto,
569 F. G. Rapid Fabrication of Silk Films with Controlled Architectures via Electrogelation.
570 *Journal of Materials Chemistry B* **2014**, *2* (31). <https://doi.org/10.1039/c4tb00833b>.
- 571 (36) Brenckle, M. A.; Partlow, B.; Tao, H.; Applegate, M. B.; Reeves, A.; Paquette, M.;
572 Marelli, B.; Kaplan, D. L.; Omenetto, F. G. Methods and Applications of Multilayer Silk
573 Fibroin Laminates Based on Spatially Controlled Welding in Protein Films. *Advanced*
574 *Functional Materials* **2016**, *26* (1). <https://doi.org/10.1002/adfm.201502819>.
- 575 (37) Hu, X.; Shmelev, K.; Sun, L.; Gil, E. S.; Park, S. H.; Cebe, P.; Kaplan, D. L. Regulation
576 of Silk Material Structure by Temperature-Controlled Water Vapor Annealing.
577 *Biomacromolecules* **2011**, *12* (5), 1686–1696.
578 https://doi.org/10.1021/BM200062A/SUPPL_FILE/BM200062A_SI_001.PDF.
- 579 (38) Luzon, M. D. Quantitative Determination of Carbohydrates With Dreywood’s Anthrone
580 Reagent. *Science (1979)* **1948**, *107* (2775), 254–255.
581 <https://doi.org/10.1126/science.107.2775.254>.

- 582 (39) Gai, T.; Tongid, X.; Hanid, M.; Li, C.; Fang, C.; Zouid, Y.; Hu, H.; Xiangid, H.; Xiang,
583 Z.; Lu, C.; Daiid, F. Cocoonase Is Indispensable for Lepidoptera Insects Breaking the
584 Sealed Cocoon. **2020**. <https://doi.org/10.1371/journal.pgen.1009004>.
- 585 (40) Guo, C.; Li, C.; Kaplan, D. L. Enzymatic Degradation of Bombyx Mori Silk Materials: A
586 Review. *Biomacromolecules*. American Chemical Society May 11, 2020, pp 1678–1686.
587 <https://doi.org/10.1021/acs.biomac.0c00090>.
- 588 (41) Cao, Y.; Wang, B. Biodegradation of Silk Biomaterials. *International Journal of*
589 *Molecular Sciences*. April 2009, pp 1514–1524. <https://doi.org/10.3390/ijms10041514>.
- 590 (42) Li, M.; Ogiso, M.; Minoura, N. Enzymatic Degradation Behavior of Porous Silk Fibroin
591 Sheets. *Biomaterials* **2003**, *24* (2), 357–365. [https://doi.org/10.1016/S0142-](https://doi.org/10.1016/S0142-9612(02)00326-5)
592 [9612\(02\)00326-5](https://doi.org/10.1016/S0142-9612(02)00326-5).
- 593 (43) Cao, Y.; Lim, E.; Xu, M.; Weng, J. K.; Marelli, B. Precision Delivery of Multiscale
594 Payloads to Tissue-Specific Targets in Plants. *Advanced Science* **2020**, *7* (13), 1903551.
595 <https://doi.org/10.1002/advs.201903551>.
- 596 (44) Zhou, Z.; Zhang, S.; Cao, Y.; Marelli, B.; Xia, X.; Tao, T. H. Engineering the Future of
597 Silk Materials through Advanced Manufacturing. *Advanced Materials* **2018**, *30* (33),
598 1706983. <https://doi.org/10.1002/adma.201706983>.
- 599 (45) Hu, X.; Shmelev, K.; Sun, L.; Gil, E.-S.; Park, S.-H.; Cebe, P.; Kaplan, D. L. Regulation
600 of Silk Material Structure by Temperature-Controlled Water Vapor Annealing.
601 *Biomacromolecules* **2011**, *12* (5), 1686–1696. <https://doi.org/10.1021/bm200062a>.
- 602 (46) Xiao Hu, †; David Kaplan, ‡ and; Peggy Cebe*, †. Determining Beta-Sheet Crystallinity
603 in Fibrous Proteins by Thermal Analysis and Infrared Spectroscopy. **2006**.
604 <https://doi.org/10.1021/MA0610109>.
- 605 (47) Smith, B. C. *An IR Spectral Interpretation Potpourri: Carbohydrates and Alkynes*.
606 Spectroscopy. [https://www.spectroscopyonline.com/view/ir-spectral-interpretation-](https://www.spectroscopyonline.com/view/ir-spectral-interpretation-potpourri-carbohydrates-and-alkynes)
607 [potpourri-carbohydrates-and-alkynes](https://www.spectroscopyonline.com/view/ir-spectral-interpretation-potpourri-carbohydrates-and-alkynes) (accessed 2021-10-11).
- 608 (48) Mendoza-Suárez, M. A.; Geddes, B. A.; Sánchez-Cañizares, C.; Ramírez-González, R. H.;
609 Kirchhelle, C.; Jorin, B.; Poole, P. S. Optimizing Rhizobium-Legume Symbioses by
610 Simultaneous Measurement of Rhizobial Competitiveness and N₂ Fixation in Nodules.
611 *Proc Natl Acad Sci U S A* **2020**, *117* (18), 9822–9831.
612 <https://doi.org/10.1073/pnas.1921225117>.
- 613 (49) Smith, C.; Hill, A. K.; Torrente-Murciano, L. Current and Future Role of Haber-Bosch
614 Ammonia in a Carbon-Free Energy Landscape †. *Energy Environ. Sci* **2020**, *13*, 331.
615 <https://doi.org/10.1039/c9ee02873k>.
- 616 (50) Ghavam, S.; Vahdati, M.; Wilson, I. A. G.; Styring, P. Sustainable Ammonia Production
617 Processes. *Frontiers in Energy Research* **2021**, *9*, 34.
618 <https://doi.org/10.3389/FENRG.2021.580808/BIBTEX>.
- 619 (51) Zvinavashe, A. T.; Mardad, I.; Mhada, M.; Kouisni, L.; Marelli, B. Engineering the Plant
620 Microenvironment To Facilitate Plant-Growth-Promoting Microbe Association. *Cite This:*
621 *J. Agric. Food Chem* **2021**, *69*, 13270–13285. <https://doi.org/10.1021/acs.jafc.1c00138>.
- 622 (52) Poole, P.; Ramachandran, V.; Terpolilli, J. Rhizobia: From Saprophytes to
623 Endosymbionts. *Nature Reviews Microbiology* **2018**, *16* (5), 291–303.
624 <https://doi.org/10.1038/nrmicro.2017.171>.
- 625 (53) Oliveira, A. N. de; Oliveira, L. A. de; Andrade, J. S. Production and Some Properties of
626 Crude Alkaline Proteases of Indigenous Central Amazonian Rhizobia Strains. *Brazilian*

- 627 *Archives of Biology and Technology* **2010**, 53 (5), 1185–1195.
628 <https://doi.org/10.1590/S1516-89132010000500024>.
- 629 (54) Krehenbrink, M.; Allan, J. A. Identification of Protein Secretion Systems and Novel
630 Secreted Proteins in *Rhizobium Leguminosarum* Bv. *Viciae*. *BMC Genomics* **2008**, 9, 55.
631 <https://doi.org/10.1186/1471-2164-9-55>.
- 632 (55) Weinbauer, K. M.-E. G. Effects of Sodium Azide on the Abundance of Prokaryotes and
633 Viruses in Marine Samples. *PLoS ONE* **2012**, 7 (5), 37597.
634 <https://doi.org/10.1371/journal.pone.0037597>.
- 635 (56) Jambeck, J. R.; Geyer, R.; Wilcox, C.; Siegler, T. R.; Perryman, M.; Andrady, A.;
636 Narayan, R.; Law, K. L. Plastic Waste Inputs from Land into the Ocean. *Science (1979)*
637 **2015**, 347 (6223), 768–771. <https://doi.org/10.1126/SCIENCE.1260352>.
- 638 (57) Zumstein, M. T.; Schintlmeister, A.; Nelson, T. F.; Baumgartner, R.; Wobken, D.;
639 Wagner, M.; Kohler, H. P. E.; McNeill, K.; Sander, M. Biodegradation of Synthetic
640 Polymers in Soils: Tracking Carbon into CO₂ and Microbial Biomass. *Science Advances*
641 **2018**, 4 (7). <https://doi.org/10.1126/SCIADV.AAS9024>.
642
643

FOR TABLE OF CONTENTS USE ONLY



We investigate the biodegradation of silk films in different environmental conditions ranging from soil to seawater, elucidating the role of the environment and protein properties on material end-life.

Synopsis

Biodegradation of silk-based films in various environmental conditions with exogenous factors and encapsulated microbes are discussed.